15

# Versatile Nanocomposite Formulation System of Non-Steroidal Anti-Inflammatory Drugs of the Arylalkanoic Acids

Mohamed R. Berber[1,2], Inas H. Hafez[2], Keiji Minagawa[2], Takeshi Mori[3] and Masami Tanaka[4]
[1]*Department of Chemistry, Faculty of Science,Tanta University*
[2]*Institute of Technology and Science, The University of Tokushima*
[3]*Department of Applied Chemistry, Kyushu University, Fukuoka*
[4]*Faculty of Pharmaceutical Sciences, Tokushima Bunri University*
[1]*Egypt*
[2,3,4]*Japan*

## 1. Introduction

Nanotechnology has shown tremendous promise in target-specific delivery of drugs in the body. Although passive and active targeted-drug delivery has addressed a number of important issues, additional properties that can be included in nanocarrier systems to enhance the bioavailability of drugs at the disease site, and especially upon cellular internalization, are very important.

Upon the support of nanotechnology, scientists in hybrid research field could deal with the combination of different substances from macroscopic to molecular level, and create novel materials with intentional functionalities. Thus, the hybridization technology can be adapted to create efficient drug nanocarriers. Hybridized drug-carriers can be made from a variety of organic and inorganic materials including biodegradable polymers and inorganic clays. The selection of material for development of nanoparticle carriers is mainly dictated by the desired diagnostic or therapeutic goal, type of payload, material safety profile, and the route of administration.

Among the various approaches for exploiting developments in drug nanotechnology, layered double hydroxide (LDH) materials offer some unique advantages, as their medical properties support their different pharmaceutical applications. By the introduction of drug-LDH nanocomposite platform, the delivery system becomes an active participant rather than passive vehicle in the optimization of drug-therapy.

In this chapter, we are going to focus on the intercalation chemistry of LDH, the different LDH nanocomposites formulation strategies, and the physical and chemical properties of drug-LDH nanocomposites. In addition, we discuss the different drug-LDH pharmaceutical applications such as drug solubility, dissolution behavior, and the delivery of some non-steroidal anti-inflammatory drugs (NSAIDs) to its active target-sites.

## 2. Layered double hydroxides (LDHs)

Driven by the high promise for new nanotechnological applications and our belief that development of biomedical science demands new advanced materials, clays are of particular interest. An interesting category of clay materials is (LDHs).

### 2.1 Structure of LDHs

LDHs are a family of natural and synthetic compounds having a general formula of $[M^{II}_{1-x}M^{III}_x(OH)_2](Y^{n-})_{x/n}\cdot yH_2O$, where $M^{II}$ and $M^{III}$ represent divalent and trivalent metal ions respectively, and $Y^{n-}$ is the anion between the layers. $M^{II}$ can be for example $Mg^{2+}$, $Ca^{2+}$, $Zn^{2+}$, $Co^{2+}$, $Cu^{2+}$; and $M^{III}$ can be $Al^{3+}$, $Cr^{3+}$, $Co^{3+}$, $Fe^{3+}$, $Mn^{3+}$. The interlayer anion $Y^{n-}$ can be $Cl^-$, $NO_3^-$, $CO_3^{2-}$, or organic anions (Boclair *et al*., 1999). LDHs are also known as hydrotalcite-like compounds due to their structural similarities to hydrotalcite mineral, or known as anionic clays. They consist structurally of brucite-like sheet with hexagonal-shaped crystallite layers as shown in the scanning electron micrograph (SEM) of Figure 1. This structured-shape is formed by the edge sharing of $[Mg(OH)_6]$ octahedral as displayed in the schematic illustration of Figure 2. The net positive charge of LDH is due to a partial substitution of $M^{2+}$ by $M^{3+}$; typically, the substitution leads to values of x in the range of 0.2 to 0.33. This positive charge is effectively dispersed uniformly across each layer (Rives, 2002). Anions are attracted into the interlayer space along with water molecules, balancing the overall positive charge with a negative one of equal magnitude. LDH materials appear in nature and can be readily prepared in the laboratory. In nature, they are formed from the weathering of basalts (Bail *et al*., 1987) or precipitation in saline water sources (Frost & Erickson, 2004). All natural LDH minerals have a structure similar to hydrotalcite, which has the formula $[Mg_6Al_2(OH)_{16}]\cdot CO_3\cdot 4H_2O$ (Cavani *et al*., 1991). Unlike clays, however, layered double hydroxides are not discovered in large scale.

### 2.2 Preparation techniques of LDHs

LDH can be prepared in the laboratory by different techniques. Coprecipitation (Miyata, 1980), anion exchange (***Liu* et al., *2006***), glycerol-effected exchange (Carlino, 1997), reconstruction (Geraud *et al*., 2007) and homogeneous precipitation (Ogawa & Kaiho, 2002). Coprecipitation is perhaps the most widely used technique of LDH. In this method, LDH is precipitated by adding a base to a stirred aqueous solution containing the metals salts ($M^{II}$ and $M^{III}$) and the desired anion. A 50 wt% solution of alkali hydroxide was found to be effective in the precipitation of pure LDH materials without impurities at the pH range 8.0-10.0. LDH systems generally prefer carbonate to most other anions. Thus, carbonate and carbon dioxide must be rigorously excluded from the medium in case of anions other than carbonate. The metal hydroxide layers nucleate and grow under stirring. Aging of the formed LDH precipitate is preferable to improve the crystallinity of LDH materials which is considered as an effective property in the stabilization of the beneficial intercalated anions. The aging process of LDH is often used as a post-treatment method and it usually performed by hydrothermal or microwave treatment techniques (Miyata, 1980).

### 2.3 Identification of LDHs and their nanocomposites

LDHs can be identified by different techniques: Powder X-ray diffraction (PXRD) is a very useful tool to analyze the crystalline structure, lattice parameters, crystal morphology, and crystal size of LDHs. This application is based on the fact that an X- ray diffraction is unique for each crystalline substance. The reflections of LDH are indexed to a hexagonal lattice

(Zou *et al*., 2007) with rhombohedral 3R symmetry. The peaks of LDH from the lower angle to the high angle are the diffraction by planes (003), (006), (009), etc. Thus, the cell parameter *c* (the thickness of one layer consisting of a brucite-like sheet and one interlayer) of LDH is usually estimated as $3d_{003}$ or $d_{003} + 2d_{006} + 3d_{009}$, and the cell parameter *a* (the mean closest metal-metal distance within a layer) can be easily calculated from the 110 reflection ($a = 2d_{110}$). XRD measurement is based on Bragg's law: $n\lambda = 2d \sin\theta$, where λ is the wavelength

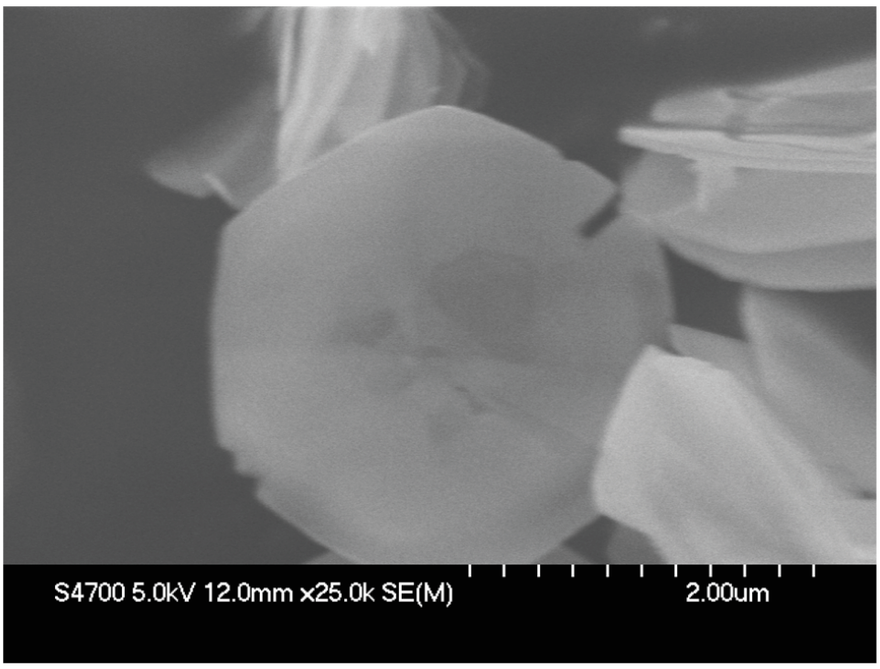


Fig. 1. SEM image of a hexagonal-shaped crystallite layer of Mg-Al LDH

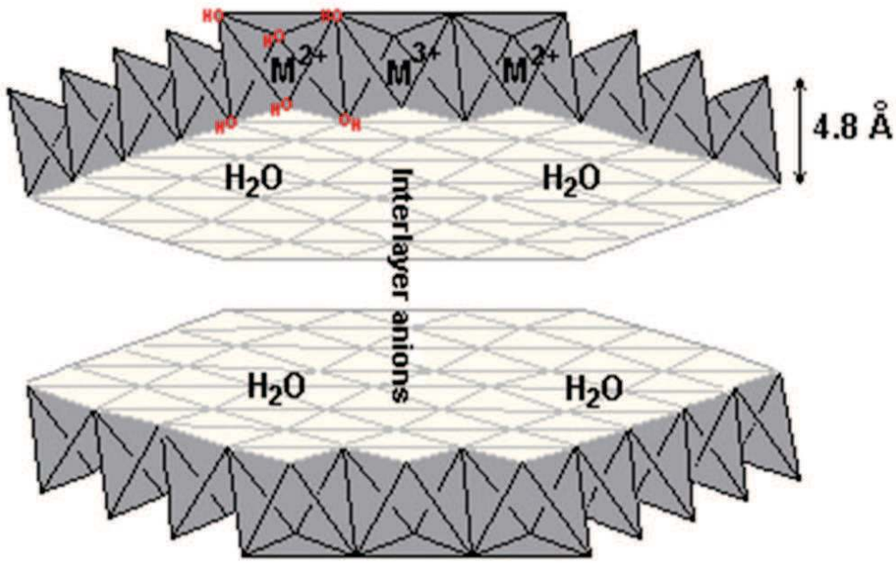


Fig. 2a. Schematic illustration of the brucite-like sheet structure of LDH; Horizontal view with a layer thickness of 4.8Å.

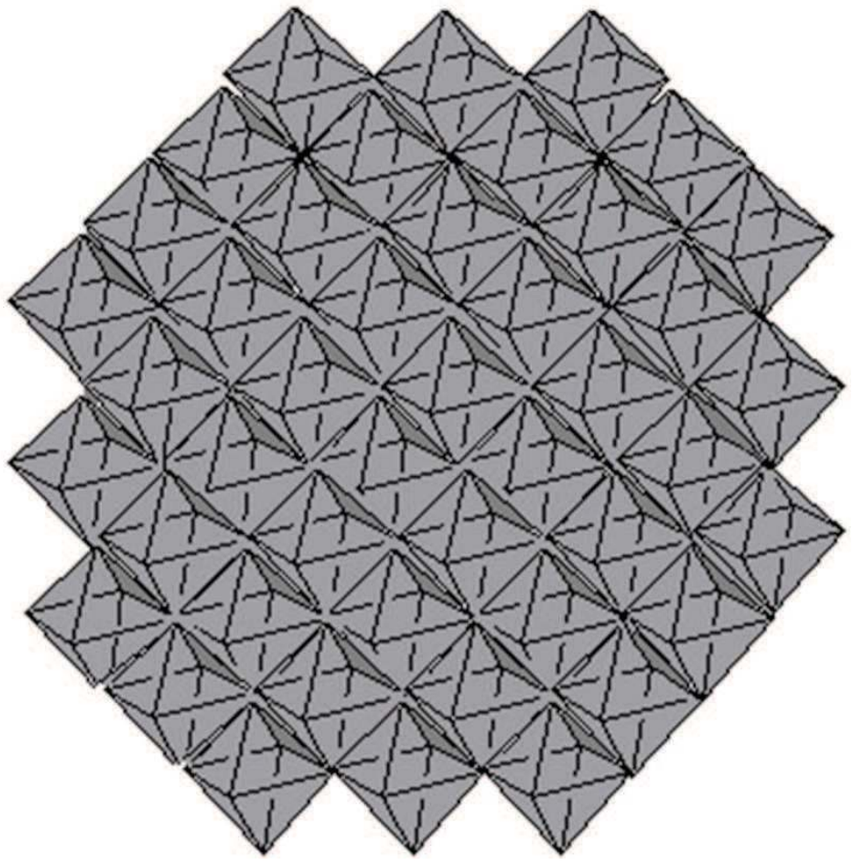

Fig. 2b. Schematic illustration of the brucite-like sheet structure of LDH; Vertical view.

of the incident X-ray beam, *d* is the spacing between each lattice, θ is the angle between the incident X-ray beam and the reflecting crystal plan, and *n* is an integer representing the order of the reflection (in practice, taken to be 1). Fourier transform infrared spectroscopy (FTIR): FTIR has been used as a tool for the evaluation of a molecule's structure by studying the vibration change occurring from the excitation of the bonds. In LDH, FTIR is used to determine the presence or absence of particular active agents in the interlayer, and to check that LDH layer material matches the expected spectrum. Since functional groups absorb at characteristic frequencies of infrared radiation, many compounds can be identified using only their spectra. Higher-quality scans of FTIR can be performed to give detailed information about the interlayer environment, to indicate the presence or absence of key functional groups in the system, to illustrate the relative orderliness of the hydroxide layers, and to determine the extent of ordering of water in the sample. We can also use FTIR to determine how much contamination (e.g. how much carbonate) is present in the system; if the LDH parent was a nitrate. We can also semi-quantitatively determine the extent of intercalation of our anion of interest. In addition, we can obtain detailed information about the extent of distortion that the intercalated anions undergo by comparing the spectra of the original compounds with those of the intercalated LDHs. Accordingly, FTIR provided valuable information on the ordering of these anions in the interlayer. Thermal analysis: the thermal gravimetrical analysis (TGA) of LDH is used to determine the thermal stability of the layered materials and also the thermal stability of the intercalated anions. Elemental

analysis for carbon, hydrogen, and nitrogen (CHN) presents a useful technique of determining the percentage of the intercalated compound where LDH does not contain these elements. Scanning electron microscopy (SEM) and transmittance electron microscopy (TEM) are used to describe the structure morphology and crystal growth of LDH, and to provide useful information about the particle size of the LDH-composite materials.

### 2.4 Properties of LDH

LHDs display unique physical and chemical properties surprisingly close to the properties of clay minerals. The most interesting properties can be summarized as follows: a- High specific surface area, that varies from a few $m^2/g$ to ~100 $m^2/g$. This property is useful in the pharmaceutical applications, gas-adsorption and purification techniques. The synthetic route of LDH has a great influence on its adsorption capacity (Malherbe *et al*., 1997). b- Memory effect, which allows a reconstruction process of LDH after calcination of the original structure by contact with solutions containing the desired anions. The calcination-reconstruction technique of LDH was used to prepare advanced nanocomposite materials of different anions. c- Anion-exchange property, this property was used to construct efficient bionanocomposites compounds of nucleosides (Choy *et al*., 2001; Lotsch *et al*., 2001), DNA (Minagawa *et al*., 2009; Xu *et al*., 2007), amino acids (Aisawa *at al*., 2006; Ajat *et al*., 2008; Chen *et al*., 2009; Reinholdt & Kirkpatrick, 2006; Wei *et al*., 2007) fatty acids (Nhlapo *et al*., 2008), sugars (Aisawa *et al*., 2003), drugs (Ladewig *et al*., 2009; Li *et al*., 2009; Tammaro *et al*., 2007; Trikeriotis & Ghanotakis, 2007; Xia *et al*., 2008; Zhang *et al*., 2009a, 2009b) and vitamins (Choy *et al*., 2004; Hwang *et al*., 2001; Tronto *et al*., 2004), through an anion-exchange mechanism of the interlayer anion of the original LDH. The exchange capacity of LDH was found to depend on the interlayer anion type. Usually LDH-$NO_3$ nanoparticles are used in the exchange process where LDH has low affinity to the interlayer anion $NO_3$ (Yahaya *et al*., 2003). d- Biomedical properties, LDH possess excellent biomedical properties such as chemical inertness, null toxicity, biocompatibility, and antacidic and antipyretic properties. Consequently, they can be used as drug matrixes, drug stabilizers during storage and drug delivery. All in all, the previously mentioned properties of LDH raise the interest of LDH applications in the different biomedical fields especially the pharmaceutical one.

## 3. Non-steroidal anti-inflammatory drugs (NSAIDs)

Many drugs used for pharmacotherapy, while having a beneficial action, can also exhibit side-effects that may limit their clinical application. Therefore, there has been a long desire to achieve safe and selective delivery of drugs to target areas in the body in order to maximize the therapeutic potential and minimize the undesired side-effects. NSAIDs (Chart 1) are classified base on their chemical structure including: Salicylatic acid derivatives (e.g. aspirin), Fenamic acid derivatives (e.g. Flufenamic acid), Acetic acid derivatives (e.g. Sulindac) and Propionic acid derivatives (e.g. Naproxen, Flurbiprofen, Suprofen, and Indoprofen).

NSAIDs are drugs with analgesic and antipyretic effects. They also produce anti-inflammatory effects when administrated in high doses. NSAIDs act by interfere with cyclooxyganase enzyme which control the production of prostaglandins responsible for inflammation and pain. However, prostaglandins have other vital functions, such as protecting the stomach from indigestion and ulcers, thus NSAIDs can have undesirable side effects in the gastrointestinal track and in some cases in the cardiovascular system.

Herein, we are going to cover the LDH nanocomposites of NSAIDs of the arylalkanoic acids derivatives. However most of NSAIDs are facing some administration problems such as low water solubility, non-target adsorption and local gastrointestinal irritation that is called direct contact effect. Thus, there is a need in-the-art for nanocomposite formulation technology to overcome the previously mentioned problems and to medicate the problems associated with prior conventional formulations such as milling and microcoating.

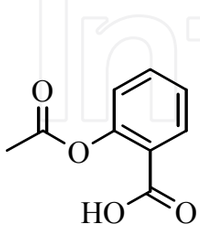

Aspirin

2-acetoxybenzoic acid

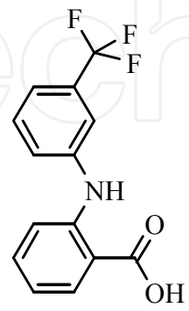

Flufenamic

2-{[3-(trifluoromethyl) phenyl]amino}benzoic acid

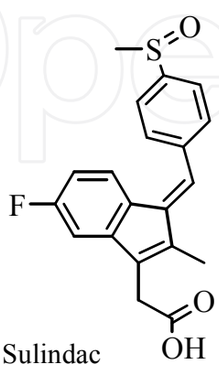

Sulindac

5-fluoro-2-methyl-1-[4-(methylsulfinyl) benzylidene]-1H-indene-3-yl acetic acid

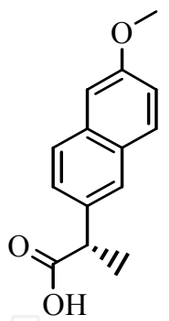

Naproxen

2-(6-Methoxy -naphthalen-2-yl) propionic acid

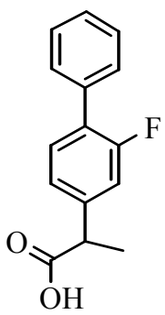

Flurbiprofen

2-(2-fluoro-4-biphenylyl) pronpanoic acid

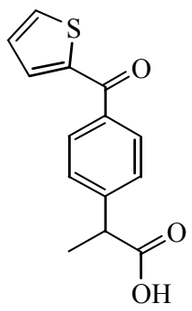

Suprofen

2-(4-thiophen-2-yl carbonyl phenyl) propanoic acid

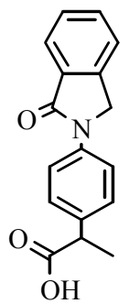

Indoprofen

2-[4-(1-oxo-1,3-dihydro-2H-isoindol-2-yl) phenyl] propanoic acid

Chart 1

### 3.1 Physicochemical properties of NSAIDs

During drug substance development the molecules are screened in nanomolar receptor assays. The molecules with the best receptor binding are selected for further pre-clinical investigations. Already at this stage, solubility is of critical importance because it estimates the poorly defined drug substances and emphasizes the drug pharmacological and toxicological profiling.

When going into humans, sufficient and well characterized solubility becomes even more critical. The solubility or dissolution of the dose ranges in the various biophysiological media to which the drug substance or formulated drug substance is expected to be reproducible and remain unchanged for the final development and eventually marketing. It is well accepted today throughout the scientific community that drug substance solubility and especially aqueous drug substance solubility is an issue for the drug discovery as well as the early and late stage pharmaceutical development process and therefore needs to be addressed perfectly during compound design and optimization.
Most of NSAIDs have low solubility or completely insoluble. To achieve a pharmacological activity of NSAIDs, the molecules must in general exhibit certain solubility in physiological intestinal fluids to be present in the dissolved state at the site of absorption. The aqueous solubility of NSAIDs is a major indicator for the drug activity in the intestinal fluids and its potential contribution to bioavailability issues. From literature, solubility or dissolution of NSAIDs can be mainly altered on two levels, through material engineering of the drug substance or through formulation approaches. Whatever route is taken to enhance or modify the solubility and/or dissolution, it needs to be a commercially viable process (Amidon *et al*., 1995; Lipinski *at al*., 1997; Lipinski, 2000). Furthermore, most classical NSAIDs have a carboxylic acid group. This acidic group can impart local gastrointestinal irritation through the direct contact with mucous membrane (Davies & Wallace, 1997; Emre, 1998). Therefore, the physicochemical properties of NSAIDs should be addressed and controlled carefully through an advanced formulation system.

### 3.2 Formulation strategies of NSAIDs

#### 3.2.1 Preliminary routes

The initial drug discovery screening is typically performed with the amorphous forms of substances in organic solvents such as dimethylsulphoxide (Semin *et al*., 2005). These formulations of high-energy forms of the substance are sufficient for the receptor and efficacy screen, but neglect any solubility characteristics of the substance at this stage and therefore cannot allow for a relevant biopharmaceutical (i.e. absorption) assessment. For the continuation of the early drug discovery program, sufficient concentration of the amorphous or crystalline drug dissolved in aqueous test media is needed for appropriate in vitro and in vivo testing. When the solubility of substances in aqueous media is limited, simple and effective formulation strategies are required.

#### 3.2.2 Conventional formulations

Particle size reduction is one of the first investigated strategies. Milling is used for particle size reduction; accordingly a particle size of about 200 nm has been achieved (Markus *et al*., 2008). However this formulation strategy raised only the drugs surface area for rapid dissolution using complicated and technically challenging processes. Later on, formulations with solubilizing agents like cyclodextrins or micellar systems were evaluated (Mura *et al*., 1995). Other systems that used solvent- or surfactant-based formulations (e.g. micro-emulsions) or solid dispersions with polyethylene glycol and with polyvinylpyrrolidone required substantial development times and might be limited due to potential excipient-related toxicity or unwanted effects on the test system (Bettinetti & Mura, 1994; Melani *et al*., 1995; Mitchell *et al*., 2003; Mura *et al*., 2001, 2003; Pignatello *et al*., 2002; Uekama *et al*., 2006). Upon that, drug-nanotechnology becomes a requirement.

Drug-delivery systems using nano- and microparticles show a clear potential for various diseases treatment. In view of advantages, the ability to target specific locations, the ability to reduce the quantity of drug that needs to be delivered to attain a particular concentration level in the vicinity of the target, and the ability to decrease the concentration of the drug at non-target sites. As a consequence, the controlled drug delivery became one of the fastest growing technologies of the pharmaceutical market.

### 3.2.3 Clay hybrid formulations

The strategy of using clay materials in drug formulation has been raised in the last century (Miyata, 1975). Several reports have evaluated the effect of the clay materials in pharmacy including biopharmaceutical objectives, modification of drug liberation, pharmacological targets to avoid or to diminish adverse effects and chemical factors. Summarizing, clays were found in solid forms of administration (tablets, capsules, granulates and dusts), liquid (suspensions and emulsions) and semisolids (ointment, pastes). In the all cases, clays fulfilled a series of chemical (stability and purity), physical (water texture, content, particles dimensions) and toxicological requirements (non-toxic, security and microbiological purity) (Flesken *et al*., 2007). In particular, the effect of clay minerals on drug solubility has received a great deal of intention. For example, the complexation of the analgesic indomethacin drug with smectite enhanced the drug-skin penetration rate and increased the drug stability as well as drug water solubility (Ito *at al*., 2001). Also, the hybridization of the poor water soluble itraconazole with smectites led to a remarkable improvement of the drug water solubility and bioavailability (Park *et al*., 2004). Furthermore, the intercalation of 5-fluorouracil into montmorillonite diminished the drug side effects through its slow release from the hybrid materials (Lin *at al*., 2002).

### 3.2.4 LDH nanocomposite formulations

The work of LDH clay materials in the field of health and pharmacy has started in the last years. Several papers have emphasized the effect of the use of LDH nanomaterials as a drug carrier. Tronto et al. (Tronto *at al*., 2001) intercalated a variety of anions of pharmaceutical interest, such as salicylate, citrate, glutamate and aspartate, using two different synthesis methods, a direct one (coprecipitation) and an indirect one (anion exchange of dodecylsulfate-LDH). Bingxin et al. (Bingxin *at al*., 2004) showed that the release of the intercalated NSAID fenbufen from LDH nanocomposites is a slow process, especially in the case of Mg/Al intercalated materials.

Recently, we described a new approach of improving drug solubility and absorption in the gastrointestinal track by using LDH nanoparticles as a drug carrier (Berber *et al*. 2008). In this work, the NSAIDs naproxen and flurbiprofen were chosen as models of poorly soluble drugs. Here, we study in details the effect of LDH nanocomposite structure on potential pharmaceutical properties of NSAIDs such as dissolution behavior, drug delivery and drug release. In addition, we emphasize the effect of LDH nanocomposite formulation technique on drug incorporation efficiency, drug preservation into the layered structure of LDH and drug thermal stability after the composite formation. For these investigations, we select some different drugs of NSAIDs such as Aspirin (ASP), Flufenamic acid (FFA), Sulindac (SUL), Suprofen (SUP) and Indoprofen (IND).

## 4. New experimental investigations

### 4.1 Materials and drugs used

Magnesium nitrate hexahydrate, aluminum nitrate nanohydrate and ASP (purity = 99.5, 98, and 99.5% respectively; Wako Pure Chemical Industries, Ltd.), FFA, SUL, NAP, FLU, SUP and IND high grades were purchased from Sigma Chemical Co., and used as received. All solutions were prepared using deionized water (18.2 MΩ/cm, produced from Milli-Q Grandient ZMQG000kt).

### 4.2 Nanocomposite formulations of the selected drugs

#### 4.2.1 Synthesis of MgAl-NO3 LDH

To a 200 mL three-necked round flask containing 30 mL of 1.0 M sodium nitrate solution was added dropwise a 50 mL solution of 8.538 g (0.0333 M) of magnesium nitrate hexahydrate and 6.249 g (0.01666 M) of aluminum nitrate nanohydrate (metal ions molar ratio of $Mg^{2+}/Al^{3+}$ = 2) with constant magnetic stirring. During the metal ion addition, the pH of the suspension was kept constant at 8.0 by adding appropriate amounts of 2.0 M KOH solution. The final volume of the preparation medium was augmented to 100 mL by deionized water. The resultant suspension was stirred at 70 °C for 24 h under $N_2$ flow. At the end of the reaction, the formed MgAl LDH material was collected by filtration (0.45 µm Millipore membrane), washed several times with deionized water, and finally freeze-dried.

#### 4.2.2 Coprecipitation technique of drug-LDH

To a 200 mL three-necked round flask, 1.0 g of the target drug was dissolved in 60 mL deionized water by adjusting the solution pH to 8.0 using 2.0 M KOH solution. A 30 mL aqueous solution containing 8.538 g $Mg(NO_3)_2 \cdot 6H_2O$ and 0.73 g $Al(NO_3)_3 \cdot 9H_2O$ ($M^{2+}/M^{3+}$ molar ratio = 2) was added dropwise with constant stirring to the drug solution. During the metal ion addition, the pH of the suspension was kept constant at 8.0 by adding appropriate amounts of 2.0 M KOH solution. The final volume of the preparation medium was augmented to 100 mL by deionized water. The resultant suspension was stirred at 70°C for 24 h under $N_2$ flow. At the end of the reaction, the formed drug-LDH material was collected by filtration (0.45-µm Millipore membrane), washed several times by 0.1 M KOH solution and subsequently deionized water until a negative test was obtained for drug in the washing medium. A UV spectrophotometer (U-3210, Hitachi, Japan) was used to check for the presence of drug (ASP, FFA, SUL, NAP, FLU, SUP and IND) in the washing medium at 235 nm, 288.0 nm, 254.0 nm, 230.5 nm, 247.0 nm, 300.4 nm and 279.0 nm respectively. Finally, the collected drug-LDH material was freeze-dried.

#### 4.2.3 Anion-exchange technique of drug-LDH

In a 100 mL round flask was dissolved 2.0 g of drug in 100 mL of deionized water by adjusting the solution pH to 8.0 using 2.0 M KOH solution. To the drug solution was added 1.0 g of $NO_3$-LDH with constant stirring. The reaction mixture was stirred at 40 °C for 7 days. After the reaction completed, the drug-LDH material was collected, washed and dried as described above in the coprecipitation technique.

#### 4.2.4 Reconstruction technique of drug-LDH

In order to prepare drug-LDH composites by reconstruction technique, the prepared $NO_3$-LDH sample was calcined at 500 °C for 4.0 h under $N_2$ flow. Depending on the memory

character of LDH, 1.0 g of the calcined LDH was dispersed in a 100 mL aqueous solution containing 1.0 g drug. The resultant suspension was stirred at 40 °C for 48 h. The obtained drug-LDH was collected, washed and finally dried as described above in the coprecipitation technique.

### 4.3 Characterization of the prepared composites

X-ray powder diffraction patterns were recorded on a Rigaku X-ray diffractometer using CuKα radiation at λ=1.5405 Å. The measurement was performed in the 2θ range 1.5-70° with a 2θ scanning step of 0.02°, a scanning step time of 5 s, a filament intensity of 40 mA, and a voltage of 150 kV. Infrared spectra (KBr disk method) were recorded on a Bio-Rad FTS 3000MX FT-IR spectrophotometer with a TGS detector in the wavenumber range of 4000-500 $cm^{-1}$ by accumulating 16 scans at 4 $cm^{-1}$ resolution. Thermogravimetric analysis (TGA) was conducted with a Shimadzu thermogravimetric analyzer (TGA-50, TA-60WS) using a platinum cell with a heating rate of 10 °C/min, under a $N_2$ flow of 20 mL/min. The scanning electron micrographs (SEM) were captured by a Hitachi FE-SEMS-4700 microscope.

## 5. Results and discussion

### 5.1 The effect of preparation technique on drug incorporation ratio

The amount of drug incorporated into LDH was calculated by using a UV quantitative method as follows. A known amount of the composite material was dissolved in 10.0 mL of 1.0 M HCl solution. The obtained solution was diluted using a phosphate buffer of pH 7.4. The drug concentration was determined from the UV-absorption peak. The drug incorporation ratio was expressed by the percentage of drug weight intercalated into a unit weight of composite. The UV method was also used to check the integrity of the target drug after the intercalation process.

Successfully, all the studied synthetic techniques showed drug-LDH composites; however the amounts of the incorporated drugs were different. The coprecipitation technique showed the highest loading ratio, while reconstruction method showed the lowest one as noted in Table 1.

| | ASP | FFA | SUL | NAP | FLU | SUP | IND |
|---|---|---|---|---|---|---|---|
| Coprecipitation technique | 53 | 58 | 45 | 52[a] | 49[a] | 49 | 51 |
| Anion exchange technique | 45 | 42 | 31 | 43 | 41 | 40 | 37 |
| Reconstruction technique | 25 | 19 | 20 | 23[a] | 21[a] | 17 | 18 |

Table 1. The determined incorporation ratios (%), [a] (Berber *et al*., 2008)

With no doubt, the preparation technique of LDH-composites affected the incorporation process of the drugs into LDH. In the coprecipitation process, the reaction medium contained the metals and the drug anion, accordingly LDH possesses high affinity to upload the drug anions and form ordered structure. In the anion exchange process, LDH is already constructed with its exchangeable inorganic anion, thus the exchange process is affected by the affinity of LDH layers to the drug charge and its size. This kind of stacking usually disturbs the layered structure of LDH. In the reconstruction process, the metal oxides of the

calcined LDH have the ability to recognize its original structure; as a consequence there is a high priority to reconstruct LDH layered structure of with the inorganic anions; especially atmospheric $CO_2$.

The X-ray patterns of Figure 3 confirmed the effect of the preparation technique on drug incorporation ratio. The absence of original LDH basal spacing peaks (pattern a) from pattern b and c indicated a successful synthesis of drug-LDH composites with single phase incorporation. The strong diffraction peaks of pattern b reflected a good crystallinity and a high ordered structure of drug-LDH composites prepared by coprecipitation technique. In the case of reconstruction technique, pattern d showed two *(003)* peaks style; one of low intensity at lower angle corresponding to the intercalated drug and the other for the $CO_3$-LDH with an interlayer distance 7.6Å. This means, the interlayer gallery of LDH contained both the drug with low content and carbonate with high content. Consequently, the method of drug incorporation has a profound influence on the drug incorporation ratio.

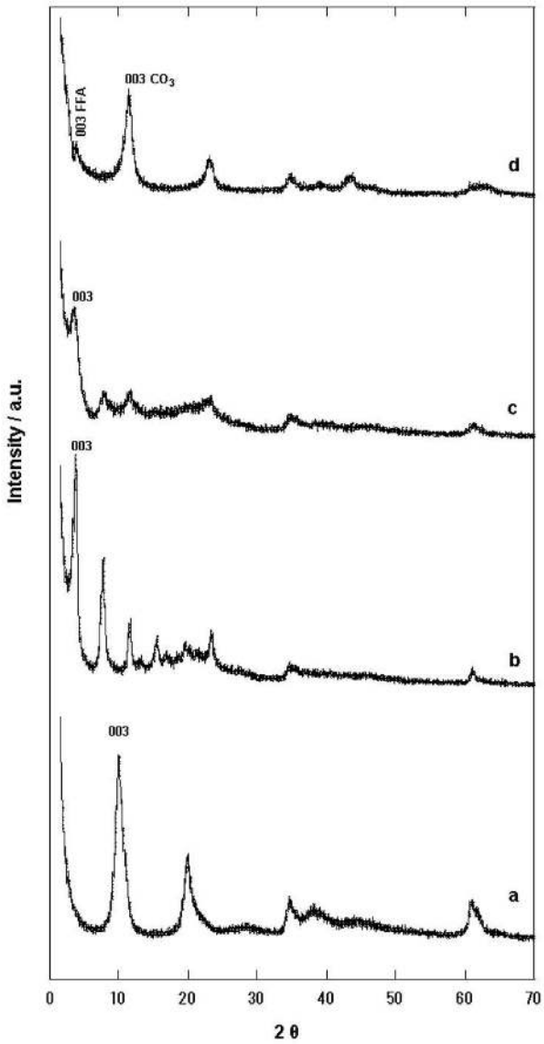


Fig. 3. X-ray diffraction patterns of $NO_3$-LDH (a), FFA-LDH coprecipitation (b), FFA-LDH anion exchange (c) and FFA-LDH reconstruction (d).

### 5.2 Nanocomposite structure of drug-LDH materials

The scanning electron microscopy was used to investigate the nanocomposite structure of the prepared materials. Figure 4 displays the SEM images of the synthesized $NO_3$-LDH material and FFA-LDH composites. Image a (inset) shows uniform and regular hexagonal platelets characteristic for LDH particles. The regularity of the LDH particles confirmed the good crystallinity recorded by X-ray measurement (X-ray section). The LDH particles size was recorded in the nanoscale. When the LDH was calcined, the hexagonal platelet structure disappeared (image b) as LDH particles lost their morphology. In the case of drug-LDH composites (images c, d and e), such LDH regular structure was demolished, and aggregates composed of small nanoparticles were observed. This aggregation process is probably due to a hydrophobic interaction of the LDH surface-adsorbed drug. The aggregates of image (e) were different from those of images (c) and (d). The aggregates were smaller in size and some regular LDH particles were observed. This difference is probably due to the applied preparation technique and the memory effect of LDH which recognize the original structure. The SEM images of the other drug-LDH materials were also recorded in the nanoscale and showed similar behaviors. Conclusively, the recorded SEM images confirmed the nanocomposite structure of synthesized drug-LDH materials.

### 5.3 X-ray analysis of drug-LDH nanocomposites

Figure 5 shows the XRD patterns of LDH, its calcined form and SUP-LDH nanocomposites prepared by previously mentioned synthetic methods. Pattern A indicated the formation of $NO_3$ form of LDH with sharp and symmetric *(00l)* reflections. Using Bragg's law ($n\lambda = 2d \sin\theta$), the basal spacing was calculated to be 8.9Å. As a result of intercalation of SUP, the basal d-spacing was expanded to 22.6 Å. The SUP-LDH nanocomposite interlayer distance was calculated by subtracting the inorganic layer thickness (4.8 Å) (Miyata, 1975) from the $d_{003}$-spacing. The determined value was 17.8 Å irrespective to the preparation technique.

The interlayer distance of SUP-LDH was larger than SUP molecular length (12.8 Å). However LDH attaches its interlayer anions through an electrostatic interaction (Costantino *et al*., 1998), we speculated that SUP molecules were stacked into LDH as a monolayer of a staggered interdigitated arrangement through the attachment of SUP carboxyl groups with the LDH positive layers, as schematically drawn in Figure 6.

Anion exchange technique (pattern c), showed a monophase drug-LDH nanocomposites. The $NO_3$ anions are fully replaced by the drug anions, showing that $NO_3$ is a good leaving group. The asymmetric broadening of the basal reflections (003 and 006) is typical of LDH composite materials with turbostratic disorder (Warren & Bodenstein, 1966; Hines *et al.*, 1997). This result clearly showed that the mechanism of anion-exchange disturbed the stacking process of the drug into the LDH layers.

Unlike coprecipitation and anion-exchange techniques, the metal oxides resulted from the calcination step are subjected to a reconstruction process. The X-ray (pattern e) showed a biphasic nanocomposites consist of the drug-LDH (lower angle; $d_{003}$ =22.6 Å) and $CO_3$-LDH (higher angle; $d_{003}$ =7.6 Å). The small amount of the intercalated drug indicated that LDH prefers to memorize its original structure (small interlayer distance) rather than incorporating large anions. In addition, carbonate anions seems to have a high priority to produce an ordered LDH structure than other anions.

To avoid reproduction of numerous X-ray diffractions, it will suffice to describe the results obtained for the other drug-LDH nanocomposites. The X-ray analysis confirmed the formation of ASP-LDH, FFA-LDH, SUL-LDH and IND-LDH nanocomposites. The X-ray patterns were generally similar to those of SUP-LDH nanocomposites. The differences were observed in the d-spacing and the interlayer distance as schematically drawn in Figure 6.

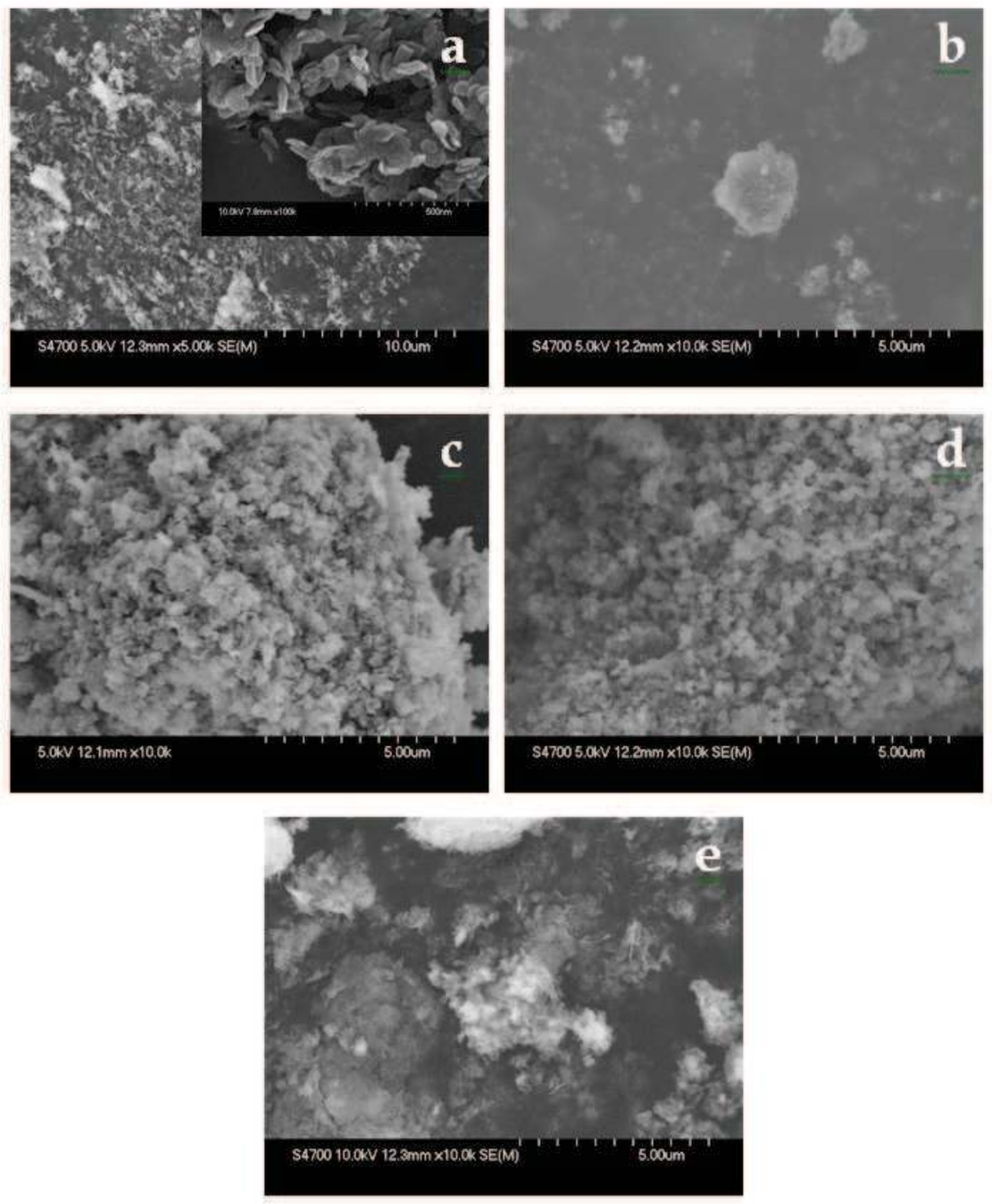


Fig. 4. SEM images of $NO_3$-LDH (a), LDH calcined (b), FFA-LDH coprecipitation (c), FFA-LDH anion exchange (d) and FFA-LDH reconstruction (e).

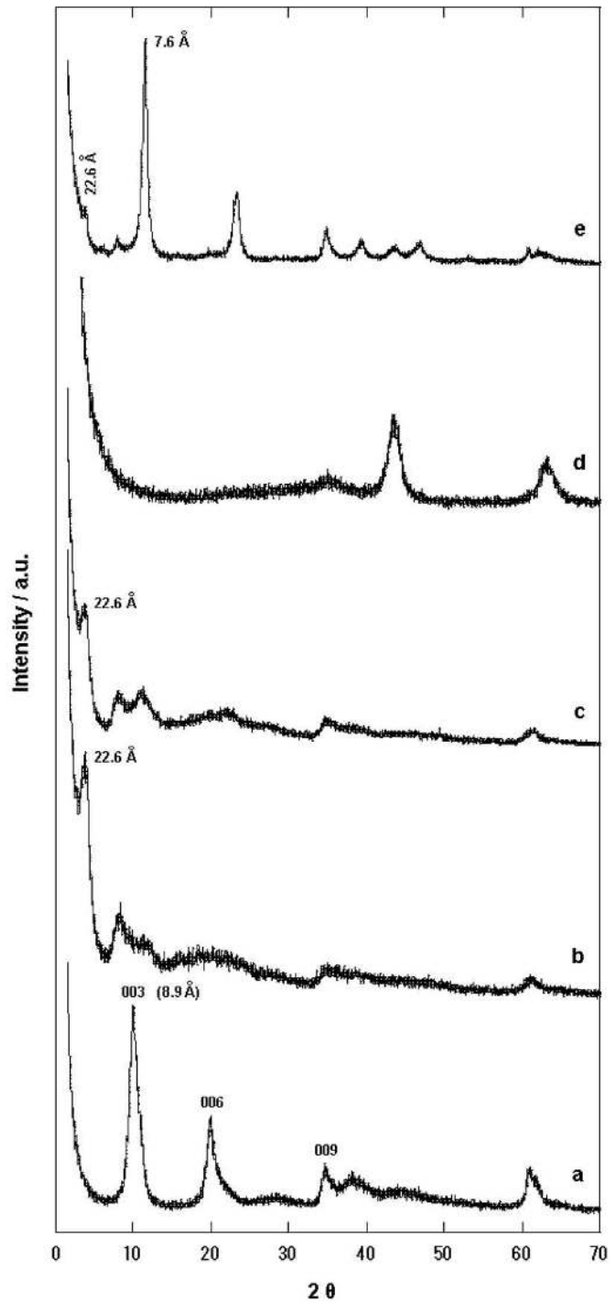


Fig. 5. X-ray diffraction patterns of $NO_3$-LDH (a), SUP-LDH coprecipitation (b), SUP-LDH anion exchange (c), calcined LDH (d) and SUP-LDH reconstruction (e).

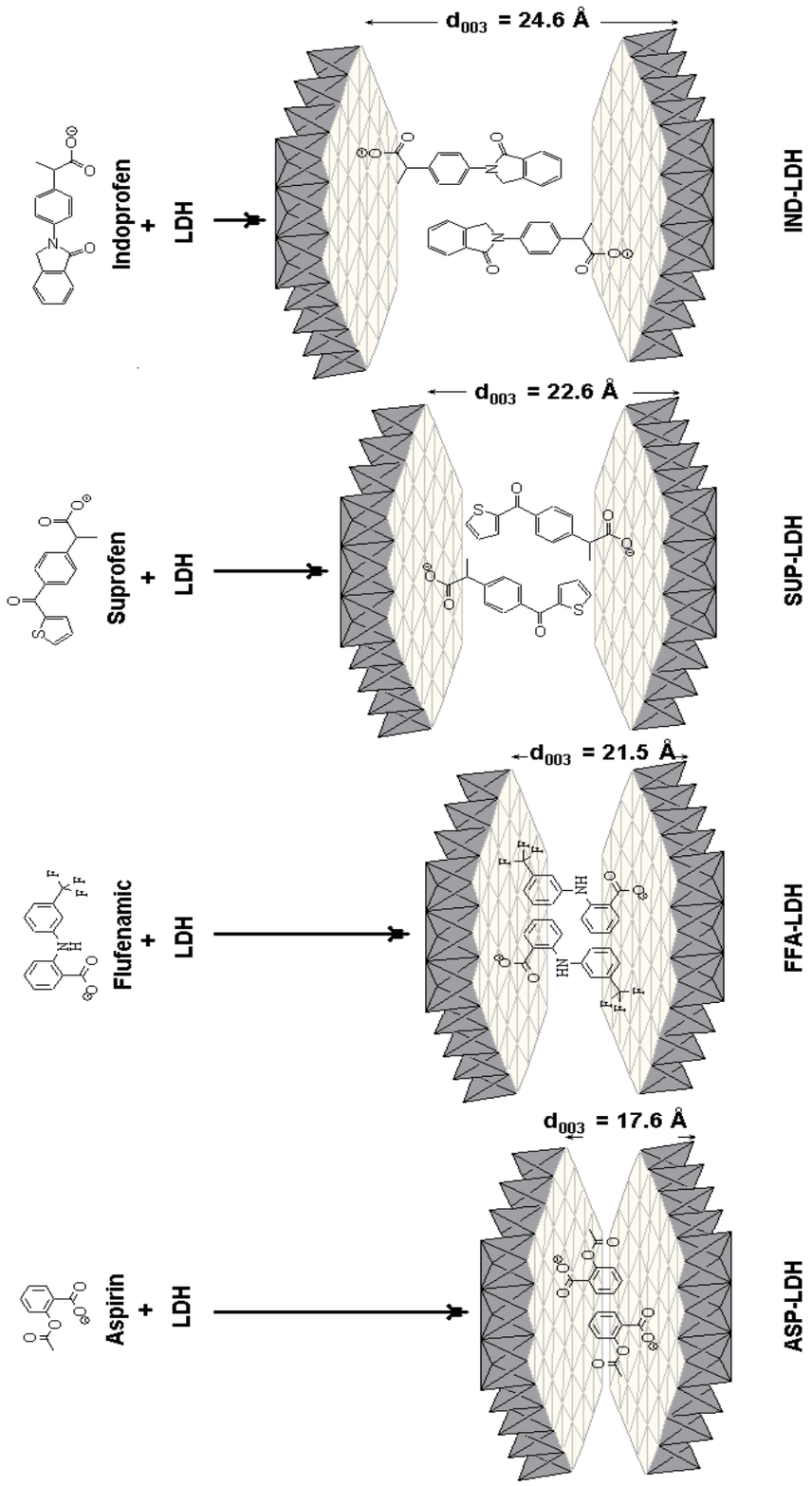


Fig. 6. Schematic illustration of intercalation process of some NSAIDs.

Accordingly, it is concluded that drug-LDH nanocomposites are produced with a high order structure, single phase incorporation of the drug with a high loading ratio in the case of coprecipitation technique.

### 5.4 Infrared spectra of drug-LDH nanocomposites

Drug-LDH nanocomposites were further characterized by FT-IR spectroscopy to verify the presence of the intercalated drugs and to gather information about the nanocomposites' molecular structure. For example, the infrared spectra of SUP-LDH nanocomposites which were prepared by different techniques are displayed in Figure 7. Figure 7a exhibited the characteristic bands of $NO_3$-LDH, in particular the lattice vibration modes ($\nu_{M-O-M}$, $\nu_{M-O}$) at 550, 630, and 780 $cm^{-1}$ (Lin *at al*., 2006) and the asymmetric stretching band of the interlayer nitrate ($\nu_{NO3}$) at 1365 $cm^{-1}$ as well as the vibration modes of the hydroxyl groups of LDH layers; bending at 960 $cm^{-1}$, deformation at 1610 $cm^{-1}$ and stretching at 3440 $cm^{-1}$ (Olanrewaju *et al*., 2000).The FT-IR spectrum of SUP (Figure 7b) showed complex features below 1520 $cm^{-1}$, which can be attributed to the bending and stretching of aromatic rings, carbon-carbon, carbon-sulfur, and carbon-oxygen bonds. The stretching vibration band of COOH group was detected at 1740 $cm^{-1}$. The weak stretching vibration modes of SUP alkyl groups ($\nu_{C-H}$) were detected between 3060 and 2870 $cm^{-1}$.

As a result of intercalation of SUP into LDH, new bands are emerged such as symmetric and asymmetric modes of $COO^-$ at 1560 and 1670 $cm^{-1}$, respectively, besides the characteristic bands of SUP and LDH. The intensities of the emerged bands suggested a dependence on the amount of the intercalated drug. The bands were sharp in the case of coprecipitation and anion exchange techniques, respectively, indicating a high loading ratio of the drug into the LDH gallery. The lack of the inorganic anions in the interlayer indicated the formation of monophase drug-LDH nanocomposites. On the other side, the reconstruction technique (spectrum e) showed the valence vibration of carbonate anion at 1410 $cm^{-1}$ (Del Arco *et al*., 1993) beside the characteristic bands of SUP, confirming the formation of biphasic nanocomposites. The presence of carbonate band in spite of the precautions taken during the preparation process indicates the high selectivity of LDH for carbonate anion (Miyata, 1980). The weak bands of the drug reflected its low interlayer contribution. In conclusion, the molecular structure information of drug-LDH nanocomposites indicated that drug molecules are intercalated into LDH gallery with different ratios depending on loading technique and are combined with LDH layers through electrostatic interactions.

### 5.5 Pharmaceutical properties of NSAIDs and their LDH nanocomposites

#### 5.5.1 Drug thermal stability

An important pharmaceutical use of LDH compounds could be drug stabilizing during storage. The active ingredient was protected by the laminar structure. In the case of the used drugs, photodecarboxylation was prevented because of the interaction of the carboxylate groups of NSAIDs and the positive layer charges. During storage, the layers of LDH supply a well-defined and relatively hydrophobic microenvironment for these guest molecules, accordingly LDH controlled the guest hydrolysis and photoreactivity (Cavani et al., 1991; Costantino & Nocchetti, 2001). Figure 8 shows the TGA and differential thermal analysis curves of LDH, SUP, and SUP-LDH prepared by co-precipitation technique.

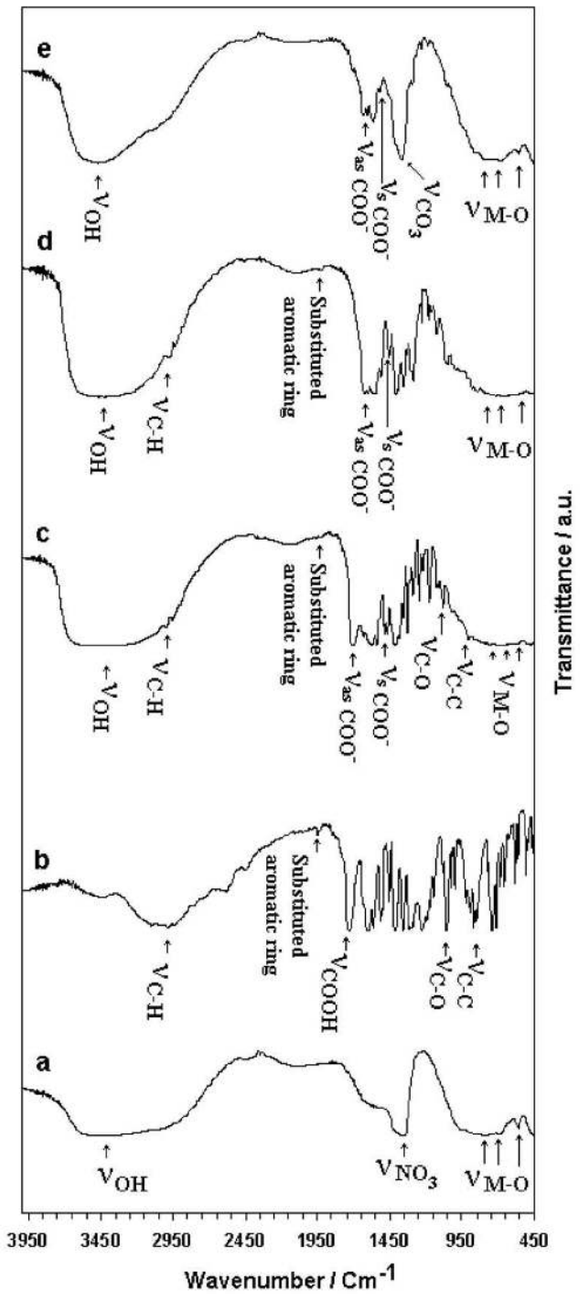


Fig. 7. Infrared spectra of LDH-$NO_3$ (**a**), SUP drug (**b**), SUP-LDH prepared by coprecipitation technique (**c**), SUP-LDH prepared by anion-exchange technique (**d**), and SUP-LDH prepared by reconstruction technique (**e**).

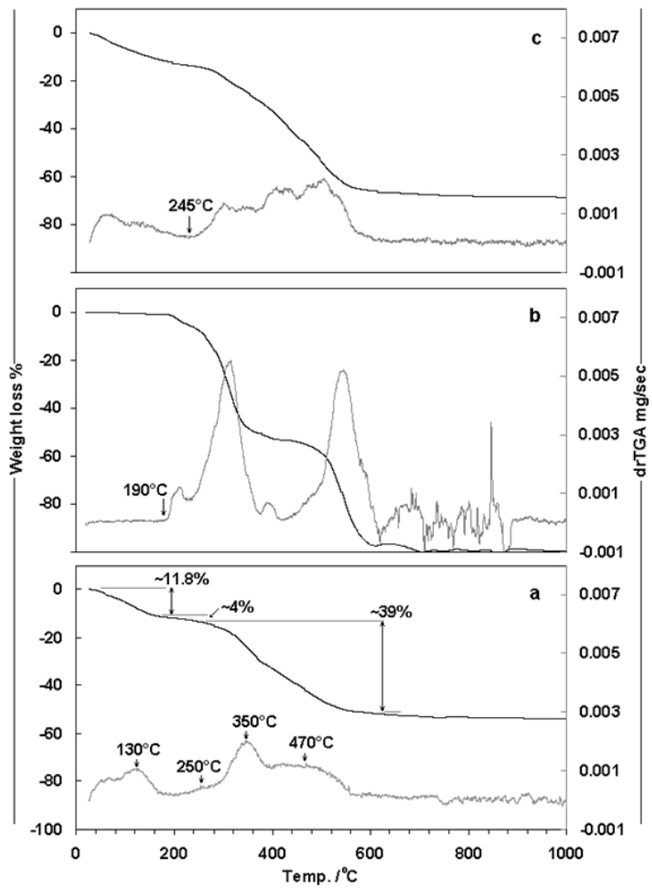


Fig. 8. Thermogravimetric analysis and differential curves of LDH-$NO_3$ (**a**), SUP drug (**b**), and SUP-LDH prepared by coprecipitation technique (**c**).

In the case of LDH (Figure 8a), the weight loss was observed to proceed mainly in three steps: ~11.8% starting from 90 °C, reaching maximum at 130 °C and ended at 170 °C (the loss of the physically adsorbed water molecules) (Darder et al., 2005), ~4% from 170 to 270 °C (the loss of the interlayer water molecules), and ~39% from 270 to 620 °C (the dehydroxylation process and the decomposition of the interlayer anions) (Lopez *et al*., 1997). The formation of MgO and $MgAl_2O_4$ oxides was observed in the TGA residue by measuring X-ray diffraction (Figure 9). The resultant oxides were in agreement with previous literature data (Labajos *et al*., 1992).

After the intercalation of SUP into LDH, the TGA curve (Figure 8c) was significantly changed. The amount of interlayer water was decreased, probably due to the hydrophobic nature of the intercalated SUP. The overall weight loss was increased from 55% to 67% in the final stage. The onset temperature of drug decomposition shifted to a higher value (from 190 °C to 245 °C). Similar changes were also observed in the TGA curves of the samples prepared by anion-exchange and reconstruction techniques. The differences were observed in the reduced weight loss which was related to the small content of the intercalated drug and the presence of carbonate as an interlayer component beside the drug in the case of reconstruction techniques. Accordingly, the stability of SUP was promoted against the thermal decomposition after the LDH nanocomposite formulation.

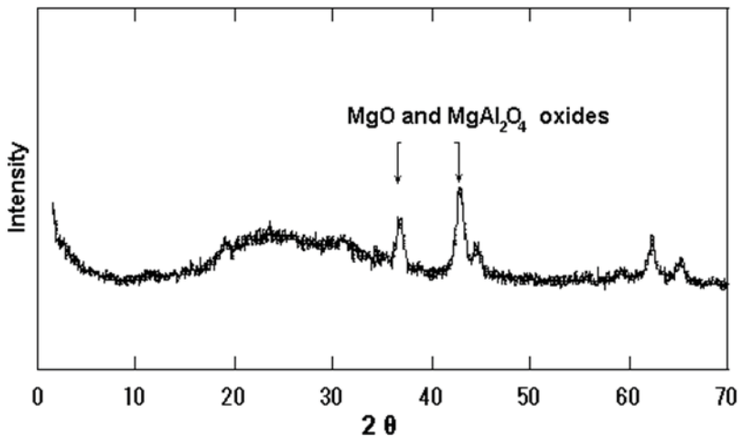


Fig. 9. X-ray pattern of TGA residue of LDH-$NO_3$

### 5.5.2 Drug delivery of NSAIDs and their LDH nanocomposites

The dissolution experiments of the pure drugs and drug-LDH nanocomposites was monitored in the following buffer mediums: buffer A as a simulated stomach solution (a 100 mL solution mixture of 100.0 mM HCl and 100.0 mM KCl; a few drops of 10.0 mM HCl solution was used to adjust the solution pH at 2.0), buffer B as a simulated duodenum solution (a 100 mL solution mixture of 100.0 mM $NaHCO_3$ and 100.0 mg NaCl; a few drops of 50.0 mM HCl solution was used to adjust the solution pH at 6.0), and buffer C as a simulated small intestine solution (a 100 mL solution mixture of 100.0 mM $NaHCO_3$ and 100.0 mg NaCl; a few drops of 50.0 mM HCl solution was used to adjust the solution pH at 8.0). The anionic buffer composition was defined on the basis of literature data (Vatier *et al*., 1992; White, 1980). By considering both of the usual daily doses of the selected drugs and the drug ratio incorporated into LDH, the release experiments were conducted with sufficient amounts of drugs-LDH nanocomposites to study the effect of LDH on drug-release properties and to ensure a good therapeutic effect. Consequently, the release experiments were performed as follows: In a round-bottom flask, a sample of 100.0 mg of drug or 200.0 mg of drug-LDH nanocomposite was dispersed in 100 mL of buffer solution, which was maintained at 36.8±0.1°C with constant agitation of 80 rpm. At appropriate time intervals, a 1.0 mL sample solution was withdrawn from the release medium and filtered by using a 0.45 μm Millipore filter unit to remove the insoluble particles. The filtrate was diluted and assayed for UV measurement. The removed aliquot was immediately replenished by the same volume of the used buffer, which was equilibrated at the same reaction temperature. The dissolution experiment of each sample in each buffer was performed in duplicates (Berber *et al*., 2010).

Figure 10 (upper panel) shows the solubility of SUP drug powder at the different mediums. The solubility was very small in buffer A (~ 6%), due to the acidic character of SUP. The drug was completely dissolved during 30 min (buffer B) and 25 min (buffer C), due to deprotonation of carboxylic acid group at high pH(s). These observations indicate the uncontrollable dissolution of SUP in the gastrointestinal tract after administration. Figure 10 (lower panel) shows the release of SUP from LDH nanocomposite prepared by coprecipitation technique. Significant change in the amount of drug dissolved was observed with time progress. Around 32%, 53% and 71% was released in a controlled process during

12 h in buffer A, B and C, respectively. The release of the intercalated SUP depended on both medium anionic species and LDH nanocomposite properties. However, LDH possesses an anion exchange selectivity for carbonate than chloride (Kaneyoshi & Jones, 1998; Miyata, 1983; Wang *et al*., 2009), the release of the drug in buffers B and C was higher than in buffer A. Additionally, the layered molecular structure of LDH limited the intercalation of the drug in two-dimensional directions. Such kind of stacking process prevents the crystallization of the drug into the gallery of LDH. As a consequence, the drug was released in an amorphous form suitable for dissolution.

The release studies of the other drugs LDH nanocomposites showed similar behaviors and changes as SUP did before and after LDH nanocomposite formation. The differences were observed only in the amounts released and releasing times. The improved release properties of the other drug-LDH nanocomposites were also related to the medium anionic species and LDH nanocomposite properties.

The question arises now: How LDH supports a controlled release process of the intercalated drug? With no doubt the exchange mechanism is the key answer. The phase boundary formed between the internal zone (drug-LDH; large d-spacing) and the external zone (exchanged LDH; small d-spacing) during the medium anion exchange process decreased the amount of drug released with time progress, consequently a controlled behavior was obtained (Kaneyoshi & Jones, 1998). At this stage and from the observations of release data, we can say that LDH nanocomposite platform enhanced the solubility of NSAIDs and diminished the drug high local concentration through a controlled release process. Furthermore, LDH material lowered the direct gastrolesivity of the NSAIDs drugs through its barrier properties.

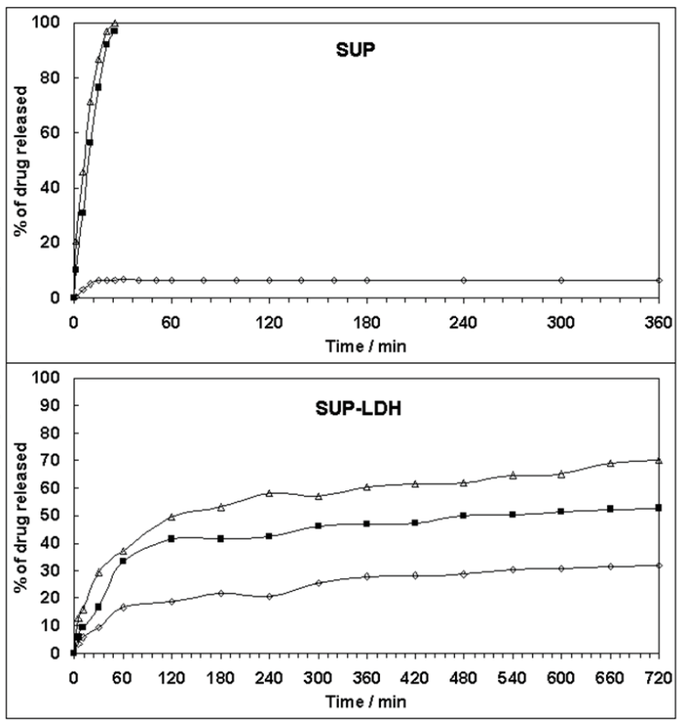


Fig. 10. Release profile of pure SUP (upper panel) and SUP-LDH nanocomposites (lower panel) in buffer A (◊), buffer B (■) and buffer C (Δ). panel

## 6. Prospects for the future of LDH

With no doubt, one of the most important advances of science and technology is the birth of nanocomposites materials. From the many significant research achievements in the past decade and the many potential practical applications, it is assumed that the prospects for nanocomposite research are very bright indeed. From commercial, industrial, and scientific point of views, clay nanocomposites are of particular interest due to their previously discussed properties. At present, even though a great deal of work on LDH materials has been carried out, still more remains to be done in order to exploit completely their potential applications.

Regarding information required for developing LDH nanocomposite science, three specific areas of research seem particularly important. The first is the optimization of present synthetic techniques or the innovation of new methodologies; however uniform LDH nanoparticles are not synthesized yet, and literature data strongly emphasized the effect of LDH nanoparticle size and its distribution ratio on the applications of LDH. In this regard, high quality basic research should be the foundation of our discipline. The directions of the basic science of LDH nanocomposites should remain open, driven by the flow of the scientific inquiry to prepare more advanced nanocomposites. Another area of focus is the establishment of new tools for the characterization of nanocomposites. It is well known that X-ray analysis is the only standard technique for the identification of clay nanocomposites. Sometimes during the analysis, peaks related to specific groups are identified by using IR spectroscopy but not by X-ray spectroscopy. Hence, much more research should be directed towards the innovation of new sensitive measurement techniques. Still another direction to consider for future LDH nanocomposite research might be the stacking mechanism of the bioactive compounds into the layers during the nanocomposite formation. Some nanocomposites are suggested to be produced in a monolayer stacking process while others are formed through a bilayer stacking process. In fact, the complete understanding of the interaction mechanism between the bioactive anions and the inorganic layers in addition to the exfoliation mechanism of the layers during the nanocomposite formation are important issues of research and will help in the preparation of more advanced nanocomposites.

Because we believe that the future of the nano-dimensional LDHs carries new innovations of utilization in the different fields, professional organizations such as high ranked universities and academic institutes are encouraged to sponsor and to focus on the LDH nanocomposite research.

## 7. References

Aisawa, S.; Hirahara, H.; Ishiyama, K.; Ogasawara, W.; Umetsu, Y. & Narita, E. (2003). Sugar-anionic clay composite materials: intercalation of pentoses in layered double hydroxide, *J. Solid State Chem.*, 174 (2), 342-348.

Aisawa, S.; Sasaki, S.; Takahashi, S.; Hirahara, H.; Nakayama, H. & Narita, E. (2006). Intercalation of amino acids and oligopeptides into Zn-Al layered double hydroxide by coprecipitation reaction, *J. Phys. Chem. Solids,* 67 (5-6), 920-925.

Ajat, M. M. M.; Yusoff, K. & Hussein, M. Z. (2008). Synthesis of glutamate- zinc-aluminium-layered double hydroxide nanobiocomposites and cell viability study, *Curr. Nanosci.*, 4 (4), 391-396.

Amidon, G. L.; Lennernäs, H.; Shah, V. P. & Crison, J. (1995). A theoretical basis for a biopharmaceutic drug classification: The correlation of in vitro drug product dissolution and in vivo bioavailability, *Pharm. Res.* 12 (3), 413-420.

Bail, C. L.; Thomassin, J.-H. & Touray, J.-C. (1987). Hydrotalcite-like solid solutions with variable $SO_4^{2-}$ and $CO_3^{2-}$ contents at 50° C, *Phys. Chem. Minerals*, 14 (4), 377-382.

Berber, M. R.; Hafez, I. H.; Minagawa, K.; Mori, T. & Tanaka M. (2010). Nanocomposite formulation system of lipid-regulating drugs based on layered double hydroxide: synthesis, characterization and drug release properties, *Pharm. Res.*, 27 (114), 2394-2401.

Berber, M. R.; Minagawa, K.; Katoh, M.; Mori, T. & Tanaka, M. (2008). Nanocomposites of 2-arylpropionic acid drugs based on Mg-Al layered double hydroxide for dissolution enhancement, *Eur. J. Pharm. Sci.*, 35 (4), 354-360.

Bettinetti, G. P. & Mura, P. (1994). Dissolution properties of naproxen in combination with polyvinylpyrrolidone, *Drug Dev. Ind. Pharm.*, 20 (8), 1353-1366.

Bingxin, L.; Jing, H.; Evans, D. G. & Xue. D. (2004). Inorganic layered double hydroxides as a drug delivery system—intercalation and in vitro release of fenbufen, *Appl. Clay Sci.,* 27 (3-4), 199-207.

Boclair, J. W.; Braterman, P. S.; Brister, B. D. & Yarberry, F. (1999). Layer anion interactions in magnesium aluminum layered double hydroxides intercalated with cobalticyanide and nitroprusside, *Chem. Mater.*, 11(8), 2199-2204.

Carlino, S. (1997). The intercalation of carboxylic acids into layered double hydroxides: a critical evaluation and review of the different methods, *Solid State Ionics*, 98 (1-2), 73-84.

Cavani, F.; Trifiro, F. & Vaccari. A. (1991). Hydrotalcite-type anionic clays: preparation, properties and applications, *Catal. Today,* 11 (2), 173-301.

Chen, Q.; Shi, S.; Liu, X.; Jin, L. & Wei, M. (2009). Studies on the oxidation reaction of cysteine in a confined matrix of layered double hydroxides, *Chem. Eng. J.*, 153 (1-3), 175-182.

Choy, J. H. & Son, Y. H. (2004). Intercalation of vitamer into LDH and their controlled release properties, *Bull. Korean Chem. Soc.*, 25 (1), 122-126.

Choy, J.-H.; Kwak, S.-Y.; Park, J.-S. & Jeong, Y.-J. (2001). Cellular uptake behavior of [gamma.-32P] labeled ATP-LDH nanohybrids, *J. Mater. Chem.*, 11 (6), 1671-1674.

Costantino, U.; Marmottini, F.; Nocchetti, M. & Vivani, R. (1998). New synthetic routes to hydrotalcite-like compounds: characterization and properties of the obtained materials, *Eur. J. Inorg. Chem.*, 10, 1439–1446.

Costantino, U.; Nocchetti. M. (2001). *Layered double hydroxides. Present and future* (V. Rives Ed.), Nova Sci. Pub. Co., Inc. New York, pp. 383-412.

Darder, M.; Blanco, M. L.; Aranda, P.; Leroux, F. & Hitzky, E. R. (2005). Bio-nanocomposites based on layered double hydroxides, *Chem. Mater.,* 17 (8), 1969-1977.

Davies, N. M. & Wallace, J. L. (1997). Non-steroidal anti-inflammatory drug-induced gastrointestinal toxicity: new insights into an old problem, J. *Gastroenterol.*, 32 (1), 127–133.

Del Arco, M.; Martin, C.; Martin, I.; Rives, V. & Trujillano, R. (1993). A FTIR spectroscopic study of surface acidity and basicity of mixed Mg, Al-oxides obtained by thermal decomposition of hydrotalcite, *Spectrochim. Acta A: Mol. Spect.,* 49 (11), 1575-1582.

Emre, M. (1998). The gastroprotective effects of tizanidine: an overview, *Curr. Ther. Res.*, 59 (1), 2–12.

Flesken, N., A.; Toshkov, I.; Naskar, J.; Tyner, K. M.; Williams, R. M.; Zipfel, W. R.; Giannelis, E. P. & Nikitin, A. Yu. (2007). Toxicity and biomedical lmaging of layered nanohybrids in the mouse, *Toxicol, Pathol.*, 35 (6), 804-810.

Frost, R. L. & Erickson, K. L. (2004). Thermal decomposition of synthetic hydrotalcites reevesite and pyroaurite, *J. Therm. Anal. Calorim.*, 76 (1), 217-225.

Geraud, E.; Bouhent, M.; Derriche, Z.; Leroux, F.; Prevot, V. & Forano, C. (2007). Texture effect of layered double hydroxides on chemisorption of Orange II, *J. Phy. Chem. Solids*, 68 (5-6), 818-823.

Hines, D. R.; Seidler, G. T.; Treacy, M. M. J. & Solin, S. A. (1997). Random stacking of a commensurate guest layer in an ordered host: NiAl layer-double-hydroxides, *Solid State Commun.*, 101 (11), 835-839.

Hwang, S. H.; Han, Y. S. & Choy, J. H. (2001). Intercalation of functional organic molecules with pharmaceteutical, cosmeceutical and nutraceutical functions into layered double hydroxides and zinc basic salts, *Bull. Korean Chem. Soc.*, 22 (9), 1019-1022.

Ito, T.; Sugafuji, T.; Maruyama, M.; Ohwac, Y. & Takahashic, T. (2001). Skin penetration by indomethacin is enhanced by use of an indomethacin/smectite, complex *J. Supramol. Chem.*, 1 (4-6), 217-219.

Kaneyoshi, M. & Jones, W. (1998). Exchange of interlayer terephthalate anions from a Mg-Al layered double hydroxide: formation of intermediate interstratified phases, *Chem. Phys. Lett.*, 296 (1-2), 183–187.

Labajos, F. M.; Rives, V. & Ulibarri, M. A. (1992). Effect of hydrothermal and thermal treatments on the physicochemical properties of Mg-Al hydrotalcite-like materials, *J. Mater. Sci.*, 27 (6), 1546-1552.

Ladewig, K.; Xu, Z. P. & Lu, G. Q. (2009). Layered double hydroxide nanoparticles in gene and drug delivery, *Expert Opin. Drug Delivery*, 6 (9), 907-922.

Li, F.; Jin, L.; Han, J.; Wei, M. & Li, C. (2009). Synthesis and controlled release properties of prednisone intercalated Mg-Al layered double hydroxide composite, *Ind. Eng. Chem. Res.*, 48 (12), 5590-5597.

Lin, F. H.; Lee, Y. H.; Jian, C. H.; Wong, J. M.; Shieh, M. J. & Wang, C. Y. (2002). A study of purified montmorillonite intercalated with 5-fluorouracil as drug carrier, *Biomaterials,* 23 (9), 1981-1987.

Lin, Y.; Wang, J.; Evans, D. G. & Li, D. (2006). Layered and intercalated hydrotalcite-like materials as thermal stabilizers in PVC resin, *J. Phys. Chem. Solids*, 67 (5-6), 998–1001.

Lipinski, C. A. (2000). Drug-like properties and the causes of poor solubility and poor permeability, *J. Pharmacol. Toxicol. Met.*, 44 (1), 235-249.

Lipinski, C. A.; Lombardo, F.; Dominy, B. W. & Feeney, P. J. (1997). Experimental and computational approaches to estimate solubility and permeability in drug discovery and development settings, *Adv. Drug Delver. Rev.*, 23 (1-3), 3-25.

*Liu, Z.; Ma, R.; Osada, M.; Iyi, N.; Ebina, Y.; Takada, K. & Sasaki, T. (2006).* Synthesis, anion exchange, and delamination of Co-Al layered double hydroxide: assembly of the exfoliated nanosheet/polyanion composite films and magneto-optical studies, J. Am. Chem. Soc., *128 (14), 4872-4880.*

Lopez, T.; Bosch, P.; Asomoza, M.; Gomez, R. & Ramos, E. (1997). DTA-TGA and FTIR spectroscopies of sol-gel hydrotalcites: aluminum source effect on physicochemical properties, *Mat. Lett.*, 31 (3-6), 311-316.

Lotsch, B.; Millange, F.; Walton, R. I. & O'Hare, D. (2001). Separation of nucleoside monophosphates using preferential anion exchange intercalation in layered double hydroxides, *Solid State Sci.*, 3 (8), 883-886.

Malherbe, F.; Forano, C. & Besse, J. P. (1997). Use of organic media to modify the surface and porosity properties of hydrotalcite-like compounds, *Micropor. Mesopor. Mater.*, 10 (1-3), 67-84.

Markus, V.; Klaus, K. & Jennifer, B. D. (2008). Dissolution enhancement of fenofibrate by micronization, cogrinding and spray-drying: comparison with commercial preparations, *Eur. J. Pharm. Biopharm.*, 68 (2), 283-288.

Melani, F.; Bettinetti, G. P.; Mura, P. & Manderioli, A. (1995). Interaction of naproxen with α-, β-, and γ-hydroxypropyl cyclodextrins in solution and in the solid state, *J. Incl. Phenom. Macro. Chem.*, 22 (2), 131-143.

Minagawa, K.; Aoki, Y.; Berber, M. R.; Mori, T. & Tanaka, M. (2009). DNA as a Component of ER Materials, *J. Phys.: Conf. Ser.*, 149(1), 012023(1-4).

Mitchell, S. A.; Reynolds, T. D. & Dasbach, T. P. (2003). A compaction process to enhance dissolution of poorly water-soluble drugs using hydroxypropyl methylcellulose, *Int. J. Pharm.*, 250 (1), 3-11.

Miyata, S. (1975). The syntheses of hydrotalcite-like compounds and their structures and physico-chemical properties-I: The systems $Mg^{2+}$-$Al^{3+}$-$NO_3^-$, $Mg^{2+}$-$Al^{3+}$-$Cl^-$, $Mg^{2+}$-$Al^{3+}$-$ClO_4^-$, $Ni^{2+}$-$Al^{3+}Cl^-$ and $Zn^{2+}$-$Al^{3+}$-$Cl^-$. *Clays Clay Miner.*, 23 (1), 369–370.

Miyata, S. (1980). Physico-chemical properties of synthetic hydrotalcites in relation to composition, *Clays Clay Miner.*, 28 (1), 50-56.

Miyata, S. (1983). Anion exchange properties of hydrotalcite-like compounds, *Clays Clay Miner.*, 31 (4), 305–311.

Mura, P.; Bettinetti, G. P.; Faucci, M. T.; Sorrenti, M. & Negri, A. (2001). Interaction of naproxen with crystalline and amorphous methylated β-cyclodextrin in the liquid and solid state, *Supramol. Chem.*, 12 (4), 379-389.

Mura, P.; Bettinetti, G. P.; Melani, F. & Manderioli, A. (1995). Interaction between naproxen and chemically modified β-Cyclodextrins in the Liquid and Solid State, *Eur. J. Pharm. Sci.*, 3 (6), 347-355.

Mura, P.; Zerroukb, N.; Menninia, N.; Maestrellia, F. & Chemtob, C. (2003). Development and characterization of naproxen–chitosan solid systems with improved drug dissolution properties, *Eur. J. Pharm. Sci.*, 19 (1), 67-75.

Nhlapo, N.; Motumi, T.; Landman, E.; Verryn, S. M. C. & Focke, W. W. (2008). Surfactant-assisted fatty acid intercalation of layered double hydroxides, *J. Mater. Sci.*, 43 (3), 1033-1043.

Ogawa, M. & Kaiho, H. (2002). Homogeneous precipitation of uniform hydrotalcite particles, *Langmuir*, 18(11), 4240-4242.

Olanrewaju, J.; Newalkar, B. L.; Mancino, C. & Komarneni, S. (2000). Simplified synthesis of nitrate form of layered double hydroxide, *Mater. Lett.*, 45 (6), 307–310.

Park, M.; Shim, I. K.; Jung, E. Y. & Choy. J. H. (2004). Modification of external surface of laponite by silane grafting, *J. Phys. Chem. Solids,* 65 (2-3), 499-501.

Pignatello, R.; Bucolo, C.; Spedalieri, G.; Maltese, A. & Puglisi, G. (2002). Flurbiprofen-loaded acrylate polymer nanosuspensions for ophthalmic application, *Biomaterials*, 23 (15), 3247-3255.

Reinholdt, M. X. & Kirkpatrick, R. J. (2006). Experimental investigations of amino acid-layered double hydroxide complexes: Glutamate-hydrotalcite, *Chem. Mater.*, 18 (10), 2567-2576.

Rives, V. (2002). Characterization of layered double hydroxides and their decomposition products, *Mater. Chem. Phys*., 7(1-3), 19-25.

Semin, D. J.; Malone, T. J.; Paley, M. T. & Woods, P. W. (2005). A novel approach to determine water content in DMSO for a compound collection repository, *J. Biomol. Screen.* 10 (6), 568-572.

Tammaro, L.; Costantino, U.; Bolognese, A.; Sammartino, G.; Marenzi, G.; Calignano, A.; Tete, S.; Mastrangelo, F.; Califano, L. & Vittoria, V. (2007). Nanohybrids for controlled antibiotic release in topical applications, *Int. J. Antimicrob. Agents*, 29 (4), 417-423.

Trikeriotis, M. & Ghanotakis, D. F. (2007). Intercalation of hydrophilic and hydrophobic antibiotics in layered double hydroxides, *Int. J. Pharm.*, 332 (1-2), 176-184.

Tronto, J.; Crepaldi, E. L.; Pavan, P. C.; De Paula, C. C. & Valim, J. B. (2001). Organic anions of pharmaceutical interest intercalated in magnesium aluminum LDHs by two different methods, *Mol. Cryst. Liq. Cryst.*, 356, 227-237.

Tronto, J.; Sanchez, K. C.; Crepaldi, E. L.; Naal, Z. K.; Stanlei, I. & Valim, J. B. (2004). Synthesis, characterization and electrochemical study of layered double hydroxides intercalated with 2-thiophenecarboxylate anions, *J. Phys. Chem.*, 65 (2-3), 493-498.

Uekama, K.; Imai, T.; Maeda, T.; Irie, T.; Hirayama, F. & Otagir, M. (2006). Improvement of dissolution and suppository release characteristics of flurbiprofen by inclusion complexation with heptakis (2,6-di-O-methyl) -β-cyclodextrin, *J. Pharm. Sci.*, 74 (8), 841-845.

Vatier, J.; Malikova-Sekera, E.; Vitre, M. T. & Mignon, M. (1992). An artificial stomach-duodenum model for the in-vitro evaluation of antacids, *Aliment. Pharmacol. Ther.*, 6 (4), 447–458.

Wang, S. L.; Liu, C. H.; Wang, M. K.; Chuang, Y. H. & Chiang, P. N. (2009). Arsenate adsorption by Mg/Al-$NO_3$ layered double hydroxides with varying the Mg/Al ratio. *Appl Clay Sci.*, 43 (1), 79–85.

Warren, B. E. & Bodenstein, P. (1966). The shape of two-dimensional carbon black reflections, *Acta Cryst.*, 20, 602-605.

Wei, M.; Guo, J.; Shi, Z.; Yuan, Q.; Pu, M.; Rao, G. & Duan, X. (2007). Preparation and characterization of L-cystine and L-cysteine intercalated layered double hydroxides, *J. Mater. Sci.*, 42 (8), 2684-2689.

White, J. F. (1980). Bicarbonate-dependent chloride absorption in small intestine: ion fluxes and intracellular chloride activities, *J. Membrane Biol.*, 53 (2), 95–107.

Xia, S.-J.; Ni, Z.-M.; Xu, Q.; Hu, B.-X. & Hu, J. (2008). Layered double hydroxides as supports for intercalation and sustained release of antihypertensive drugs, *J. Solid State Chem.*, 181 (10), 2610-2619.

Xu, Z. P.; Walker, T. L.; Liu, K.-l.; Cooper, H. M.; Lu, G. Q. M. & Bartlett, P. F. (2007). Layered double hydroxide nanoparticles as cellular delivery vectors of supercoiled plasmid DNA, *Int. J. Nanomed.*, 2 (2), 163-174.

Yahaya, A. H.; Bin-Hussein, M. Z. & Seh, W. S. (2003). Ion exchange study of carbonate, nitrate and dioctyl sulfosuccinate with anthraquinone-2-sulphonate encapsulated in inorganic layered structures, *J. Phys. Chem. Solids*, 64 (7), 1113-1118.

Zhang, H.; Pan, D. & Duan, X. (2009). Synthesis, characterization, and magnetically controlled release behavior of novel core-shell structural magnetic ibuprofen-intercalated LDH nanohybrids, *J. Phys. Chem. C.*, 113 (28), 12140-12148.

Zhang, H.; Pan, D.; Zou, K.; He, J. & Duan, X. (2009). A novel core-shell structured magnetic organic-inorganic nanohybrid involving drug-intercalated layered double hydroxides coated on a magnesium ferrite core for magnetically controlled drug release, *J. Mater. Chem.*, 19 (19), 3069-3077.

Zou, K.; Zhang, H. & Duan, X. (2007). Studies on the formation of 5-aminosalicylate intercalated Zn−Al layered double hydroxides as a function of Zn/Al molar ratios and synthesis routes, *Chem. Eng. Sci.*, 62 (7), 2022-2031.

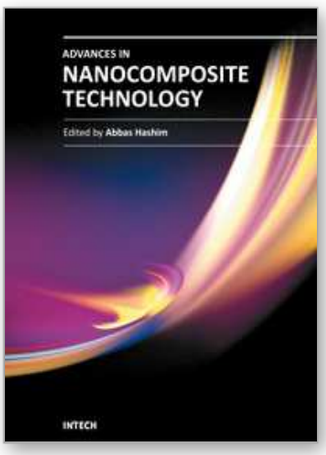


**Advances in Nanocomposite Technology**

Edited by Dr. Abbass Hashim

ISBN 978-953-307-347-7
Hard cover, 374 pages
**Publisher** InTech
**Published online** 27, July, 2011
**Published in print edition** July, 2011

The book â€œAdvances in Nanocomposite Technologyâ€ contains 16 chapters divided in three sections. Section one, â€œElectronic Applicationsâ€, deals with the preparation and characterization of nanocomposite materials for electronic applications and studies. In section two, â€œMaterial Nanocompositesâ€, the advanced research of polymer nanocomposite material and polymer-clay, ceramic, silicate glass-based nanocomposite and the functionality of graphene nanocomposites is presented. The â€œHuman and Bioapplicationsâ€ section is describing how nanostructures are synthesized and draw attention on wide variety of nanostructures available for biological research and treatment applications. We believe that this book offers broad examples of existing developments in nanocomposite technology research and an excellent introduction to nanoelectronics, nanomaterial applications and bionanocomposites.

**How to reference**

In order to correctly reference this scholarly work, feel free to copy and paste the following:

Mohamed Berber, Inas Hafez, Keiji Minagawa, Takeshi Mori and Masami Tanaka (2011). Versatile Nanocomposite Formulation System of Non-Steroidal Anti-Inflammatory Drugs of the Arylalkanoic Acids, Advances in Nanocomposite Technology, Dr. Abbass Hashim (Ed.), ISBN: 978-953-307-347-7, InTech, Available from: http://www.intechopen.com/books/advances-in-nanocomposite-technology/versatile-nanocomposite-formulation-system-of-non-steroidal-anti-inflammatory-drugs-of-the-arylalkan

INTECH
open science | open minds

**InTech Europe**
University Campus STeP Ri
Slavka Krautzeka 83/A
51000 Rijeka, Croatia
Phone: +385 (51) 770 447
Fax: +385 (51) 686 166
www.intechopen.com

**InTech China**
Unit 405, Office Block, Hotel Equatorial Shanghai
No.65, Yan An Road (West), Shanghai, 200040, China
中国上海市延安西路65号上海国际贵都大饭店办公楼405单元
Phone: +86-21-62489820
Fax: +86-21-62489821

IntechOpen